Chapter

Transition Metal Oxide-Based Nano-materials for Energy Storage Application

Apurba Ray, Atanu Roy, Samik Saha and Sachindranath Das

Abstract

With improvement of global economy, the fatigue of energy becomes inevitable in twenty-first century. It is expected that the increase of world energy requirements will be triple at the end of this century. Thus, there is an imperative need for development of renewable energy sources and storage systems. Among various energy storage systems, supercapacitors are ascertained one of the most significant storage devices. But the development of supercapacitor devices with high power and energy density are the greatest challenges for modern research. In this article, transition metal oxides such as TiO_2-V_2O_5, $NiMn_2O_4$ etc. with porous structure are considered as high performance supercapacitors electrode. The effects of its structural, morphological and electrochemical properties have been studied extensively. A TiO_2-V_2O_5 and $NiMn_2O_4$ based electrode delivered specific capacitance of 310 and 875 F g^{-1}, respectively at a scan rate 2 mV s^{-1}. This TiO_2-V_2O_5 based asymmetric supercapacitor also exhibits excellent device performance with specific energy 20.18 W h kg^{-1} at specific power 5.94 kW kg^{-1}, and retained 88.0% specific capacitance at current density of 10 A g^{-1} after 5000 cycles.

Keywords: supercapacitor, transition metal oxides, nanostructure, energy density, power density

1. Introduction

Rapidly depleting level of fuel reservoir along with the increasing effect of environmental pollution are the two most important concerns of twenty-first century. The rate at which the fossil fuel is being consumed today, it will take around 40 more years to run all the known oil deposits dry leaving the whole world into complete darkness. Fossil fuel is a very rich form of energy containing around 30–50 MJ of energy per kilogram. Combustion of fossil fuels results in the emission of CO_2, CH_4, N_2O etc. in the atmosphere which trap the solar radiation in the atmosphere [1, 2]. Although the natural trapping of solar radiation is vital for all the lives on the earth but due to excessive emissions of these gases the earth is getting hotter. According to the study conducted by NASA's Goddard institute, the Earth's average temperature has risen by 0.8°C since the beginning of the industrial revolution. Although this increment may seem very small but the alarming fact is that a little

more increase in the global temperature will cause the polar ice caps and glaciers to melt, causing the sea level to rise flooding the costal lines [3]. In order to sustain human growth these issues have to address as soon as possible. To reduce the world's hunger for fossil fuels while maintaining the same life standards we have to focus on the alternative green energy sources like solar, wind, tidal etc. Although these sources have the ability to meet the world's energy requirements but the intermittent nature of these energy sources is an unavoidable problem which significantly stimulates the motivation of research on the energy storage systems. Today a variety of energy storage and conversion devices are available such as batteries, conventional capacitors, fuel cell and supercapacitors etc. But among such energy storage systems electrochemical capacitors or supercapacitors have drawn attention as one of the most promising energy storage systems because of their high power density, short charging time and long life span although having moderate energy density 10–15 mWh/g which is still very less compared to batteries. Different research groups in the world are trying to improve the energy density and overall life span of the device by suitably choosing different electrode materials [4–8].

2. Brief history of supercapacitor

Electrical charge storage by a surface was first discovered from the phenomena of rubbing amber with fur which attracts dust in ancient age. Invention of the Leiden jar in 1757 is the first developed technology for capacitor. This Leiden jar was further improved to flat capacitor by Banjamin Franklin. This resulted in the reduction of volume as well as increase in reliability and convenience. In the late nineteenth century Helmholtz solved the electrical charge storage by a capacitor by using Faraday's law. He proved the existence of two parallel sheets of opposite charges on the surface of metal and the solution side. He proposed the model of charge/ion distribution near metal surface. It is the foundation stone for the development of fundamental aspects of capacitive technology as well as the quantitative science which describe the nature of electrostatic behavior. In the General Electric Laboratories (1957), they have developed a capacitor by using two porous carbon electrodes and aqueous electrolyte. Later it is known as electrochemical double layer capacitor. They got the U.S. Patent for this (US Patent 2,800,616). Almost a decade later (1966), Standard Oil of Ohio's (SOHIO) scientists and engineers have developed the modern electrochemical supercapacitor (SC) capacitor using porous carbon and non-aqueous electrolyte [9–12]. The non-aqueous electrolyte enables to have wide potential window for SC, which results in the increase in storage capacity. SOHIO sold this technology to Nippon Electric Company (NCE, Japan) and they used it commercially for the first time as the backup power for computer memory and also named as the supercapacitor. Presently, NEC/TOKIN, ELNA, Maxwell Technologies, Panasonic and several other companies invest in the development of supercapacitors. In 2004, the worldwide market of supercapacitor was 100 million US dollars, while the worldwide sales of supercapacitor reached to 400 million US dollars by the end of 2010. It was estimated that the market of supercapacitor will rise to 2 billion US dollars by 2020 [13–15].

3. Different types of supercapacitor

The importance of supercapacitor as an energy storage was significantly increased in the last decade of twentieth century and it witnessed significant advances in the field. Several works by Conway et al. and others [United States Pat., 1996] have investigated and identified the underlying chemistry and developed the

model for charge storage. Due to the charge storage mechanism, supercapacitors are categorized into two different types, electrochemical double layer capacitors (EDLCs, non-Faradic electrostatic storage) and pseudocapacitors (Faradic, redox reaction based capacitors). In addition, there is another class of supercapacitors known as hybrid supercapacitors which is the combination of both storage mechanisms. In this chapter, the storage mechanism, electrode materials, electrolytes of different supercapacitors will be discussed.

3.1 Electrochemical double layer capacitor (EDLC)

EDLCs have a similar structure to that of conventional capacitors except the dielectric is being replaced by electrolyte. Two highly porous carbon electrodes are separated by a porous separator and electrolyte. The energy storage mechanism of EDLC relies on the non-Faradic process i.e. electrostatic adsorption ions at the electrode/electrolyte interface. During the charging, the positive and negative ions of the electrolyte are separated and adsorbed by negative and positive electrodes, respectively. The energy storage mechanism is based on the formation of double layers of electrolyte ions at the interface of electrode and electrolyte. This is similar to the parallel plate capacitor and the capacitance of EDLC can be calculated by Eq. (1)

$$C = \frac{\varepsilon \varepsilon_0 A}{d} \tag{1}$$

where, C is the capacitance, ε_0 is the dielectric constant in vacuum, ε is the dielectric constant of the double layer, A is the area of the electrode and d is the thickness of double layer. Various models have been proposed to explain the formation of double layer. In 1853, Helmholtz first introduced the idea of double layer. When a charged conductor is placed in contact with electrolyte, the distribution of electric charges will be modified. Two layers of opposite charges will be formed at the interface of electrode and electrolyte. These two layers are separated by molecular dimensions but there is no exchange of ions between the layers. Hence the capacitance of the double layer can be obtained from the aforementioned Eq. (1). This model is widely used to explain the storage of supercapacitor. But this model did not taken care of the effects of ions behind the first layer of the ions at the electrode/electrolyte interface. Various carbonaceous materials (activated carbons, graphene, CNT etc.) store charges via EDLC mechanism. Carbon based materials were the first choice for the commercial applications because of their rapid response, good electrical conductivity, high chemical stability, non-toxicity, high abundance and simplicity of design. Carbonaceous materials have very high specific surface area (1000–3500 $m^2\ g^{-1}$) which is very useful for the charge storage since EDLC is a surface dependent phenomenon. But with the increase of specific surface area and porosity the stability and conductivity of the material decreases. In spite of this, mesoporous nature with high specific surface area is very much important for its application as an active electrode [9, 16–18].

3.2 Pseudocapacitor

Another class of supercapacitor is pseudocapacitors which rely on the reversible redox reaction or Faradic reaction to store energy. Mainly transition metal oxides (e.g. ruthenium oxide, nickel oxide, manganese oxide, vanadium pent oxide etc.) and conducting polymer (polyaniline, polypyrrole, PEDOT:PSS, etc.) belongs to this group. Close surface to the electrolyte take part in redox reactions and this process can be classified into three distinct types which are underpotential deposition (adsorption pseudocapacitance), redox pseudocapacitance and intercalation

pseudocapacitance. Underpotential deposition arises when reversible adsorptions as well as removal of atoms occur at metal surface in two dimensional Faradic reactions. Redox pseudocapacitance exists when reversible redox reactions taken place at the electrode surface. In case of intercalation pseudocapacitance, ions are electrochemically intercalated into the structure of redox materials.

Although these three mechanisms are physically different from each other but they can be electrochemically governed by the Nernst equation. According to this equation, if the reaction potential E can be approximated by a linear function of $(1 + Q_r)/Q_r$, the specific capacitance can be obtained from Eq. (2)

$$C_m = \frac{nF}{mE}\left(\frac{1+Q_r}{Q_r}\right) \tag{2}$$

where, n is the number of electron, F is the Faraday constant, m is the molecular weight of active electrode and Q_r is the reaction quotient. Transition metal oxides are chosen as the active materials for supercapacitor electrode and they store charge via Faradic or redox mechanism. They exhibit large theoretical specific capacitance with multiple valence states which enables them one of the most studied materials group in the field of supercapacitor [1, 19].

3.3 Hybrid supercapacitor

Hybrid supercapacitors are third type of supercapacitors which combine the features of both EDLCs and pseudocapacitors. The electrodes of hybrid supercapacitors are made with composite materials that include EDLC materials (carbonaceous materials such as activated carbon, graphene, CNT etc.) and pseudocapacitive materials (transition metal oxides and conducting polymers). There can also be asymmetric supercapacitor with one pseudocapacitive electrode and another EDLC electrode or hybrid electrode or vice-versa. Several binary and ternary composite based on polymer and CNTs have been prepared for electrochemical capacitive energy storage application. They offer large specific capacitance compare to individual one, which is due to the strong interaction between polymer and CNTs. Gupta and Miural were the first to propose that SWNT/PANI composite can be effectively used as the electrodes for supercapacitors. The highest specific capacitance value of 463 F g^{-1} was obtained for 27 wt% CNT.

4. Electrolytes

Besides the electrodes, another most important factor which can expressively influence the electrochemical performance of supercapacitor device is electrolyte. Generally, electrolyte exists in inside the separator as well as inside the active material layers. The important factors for an electrolyte are one wide potential window which is key factors to achieve higher energy density and the other is the high ionic concentration, low resistivity, low viscosity etc. which can also influence the power density of the supercapacitor device. There are three types of electrolyte usually used in supercapacitors: aqueous electrolyte, organic electrolytes and ionic electrolytes. Aqueous electrolytes (such as H_2SO_4, KOH, Na_2SO_4, HCl, NaCl and NH_4Cl aqueous solution and so on) limit the cell voltage window of supercapacitor to typically 0–1 V due to their low electrochemical stability, which effectively reduces the energy density of the cell. It can also provide a higher ionic concentration with conductivity up to 1.0 S cm^{-1}. Supercapacitors containing aqueous electrolyte may exhibit higher charge storage capacity but the main drawback is in terms of improving both energy and power densities due to their narrow working

potential window. To overcome this drawback now-a-days researchers are interested in using organic electrolytes as the main advantage of an organic electrolyte is it can provide wide potential window ~3.5 V. Since the energy density of a supercapacitor is directly proportional to the square of the cell voltage thus the organic electrolyte is much more suitable compared to other electrolytes. Among various organic electrolytes, acetonitrile and propylene carbonate (PC) are commonly used solvents. Propylene carbonate (PC)-based electrolytes are eco-friendly and can offer a wide electrochemical window, a wide range of operating temperature, as well as good electrical conductivity. In addition to promising advantages, the high cost, safety concern and toxic in nature still limit their commercial applications. Ionic electrolyte also known as room temperature molten salts-ionic liquids is one of the most promising electrolytes for the next generation energy storage application. Ionic electrolyte have lots of advantages such as high thermal stability, non-toxicity, non-flammability, high electrochemical stability and various combination of choices of cations and anions. But the low ionic conductivity at room temperature of ionic liquids is a great issue for practical application [20, 21].

5. Method for calculation of specific capacitance

The cyclic voltammetry (CV) curve of active working electrode materials measured in any suitable electrolyte solution (organic, ionic and aqueous electrolyte) epitomizes the total stored charge which ascends from both Faradic and non-Faradic process. The presence of oxidation/reduction peaks in CV curve represents the Faradic charge transfer reaction between electrolyte and electrode material. The total charge stored in electrode material can be calculated using Eq. (3):

$$C_m = \frac{i}{2mv} \tag{3}$$

where m and ν are the mass of the electroactive material and potential scan rate, respectively. Current (i) can be obtained by integrating the area of the curves using Eq. (4)

$$i = \frac{\int_{V_a}^{V_c} i(v)dv}{V_c - V_a} \tag{4}$$

where V_a and V_c are the lowest and highest voltage of the potential range, respectively.

The specific capacitance value of the material can also be calculated from Galvanostatic charge discharge (GCD) profiles by using Eq. (5)

$$C_m = \frac{i}{m\left(-\frac{dV}{dt}\right)} \tag{5}$$

where 'i' is the current applied, dV/dt is the average slope of the discharge curve and m is the mass of active electrode materials [22, 23].

6. TiO_2-V_2O_5 nanocomposites as supercapacitor applications

Among various transition metal oxides, vanadium oxides (V_2O_5) also known as vanadium pentoxides have already been studies as a promising supercapacitor electrode material for energy storage application due to its excellent physical properties,

layered structure, non-toxic in nature, easy synthesis process, presence of several oxidation states (+2 to +5) and high specific capacity. But its low electrical conductivity limits its practical device application. The charge storage mechanism of a supercapacitor strongly depends on the surface properties of the electrode materials so the nanomaterial is suitable for electrode fabrication. Nanomaterial possesses high surface area along with high surface energy but the aggregation of nanoparticles is the most challenging problem. This effectively increases the strain for electrolyte ions diffusion within the nanoparticles at the surface of the electrode. Therefore, people are working to design and fabricate three-dimensional (3D), ordered and mesoporous nanomaterial to overcome such type of problem. There are four fundamental steps to control the charge storage behaviors of nanomaterials: (i) electron hopping between two nanoparticles; (ii) electron hopping within single nanoparticle; (iii) electron hopping between active electrode materials and current collectors; finally (iv) diffusion of proton within nanoparticles. It is well known that the proton diffusion and electron hoping within the nanoparticles are intrinsic properties of nanoparticles but the resistance due to intra-particle electron hopping can be diminished by loading it on a stable metal oxide [2]. It has also been observed practically that the loading on a stable metal oxide affects the increase of diffusion barrier of proton within the active materials and which follows the loss of effective sites. Because of the combination of TiO_2 with V_2O_5 Ti-O-V bonds are formed instead of metal-metal bonds which can result in an overall improvement of electrochemical activity and chemical stability due to the drop in the intra-particle electron-hopping resistance. Thus, TiO_2-V_2O_5 nanocomposite can be a promising candidate for supercapacitor electrode in the near future. In this work, interconnected mesoporous TiO_2-V_2O_5 nanocomposite has been synthesized which demonstrate tube like structure. The as synthesized electrodes of TiO_2-V_2O_5 composite demonstrate kinetically fast charge-discharge properties along with long-cycle stability, which are commanding properties for supercapacitors [12, 23].

6.1 Morphological analysis

The field emission scanning electron microscopy (FESEM) images (**Figure 1(a)**) of TiO_2-V_2O_5 nanocomposite shows ordered array of tube-like mesoporous structure. Because of large surface area, these mesoporous tube-like nanostructure can provide large number of active sites for competent ion diffusion. Due to increase in the contact area of the material with electrolyte ions, such type of surface improves the electrochemical activities of the electrode material. The active specific surface

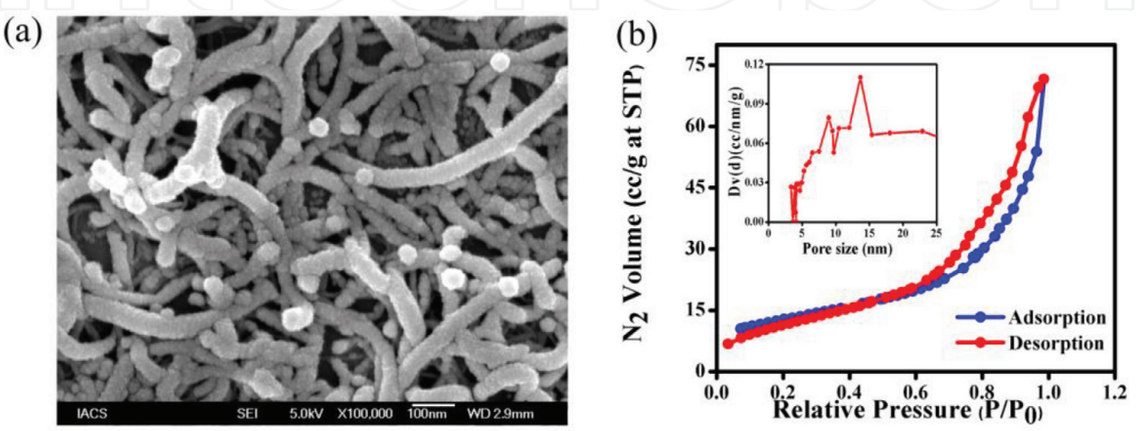

Figure 1.
(a) FESEM image of TiO_2-V_2O_5 composite; (b) N_2 adsorption-desorption isotherms and pore size distribution curve (inset) of as prepared TiO_2-V_2O_5.

area of this material has also been further characterized by nitrogen adsorption and desorption BET surface area measurement. The adsorption-desorption plot (**Figure 1(b)**) of the composite reveals the typical type-IV isotherm and also demonstrates the mesoporous nature of TiO_2-V_2O_5 nanostructure. The specific surface area calculated from the BET measurement is around 44m^2 g^{-1}. This large surface area provides large contact area between the electrode/electrolyte interface enabling fast ion transfer which can improve the electrochemical performances of the electrode material. The corresponding pore size distribution of this electrode material measured from the isotherm BJH model is shown in **Figure 1b** (inset). The average pore size for this TiO_2-V_2O_5 nanostructure is around 8.90 nm, which implies that the material possesses a mesoporous like wide pore size distribution.

6.2 Electrochemical analysis

The CV curves of TiO_2-V_2O_5 composite (**Figure 2(a)**) with different scan rates (2, 10, 50 and 100 mV s^{-1}) signify a good electrochemical redox process. There is no O_2 or H_2 gas evolution observed at the ends of the potential windows which infers that this electrode can work in the wide potential window (−0.5 to +1.3 V) without suffering any degradation. The total charge stored in the electrode due to the redox reactions and pseudocapacitive behavior can be obtained from the total area enclosed by the CV curve for a particular scan rate. Same nature of CV curve for all scan rates reveals the good electrochemical performance of the electrode. This composite offers maximum specific capacitance of 310 F g^{-1} at a scan rate 2 mV s^{-1}. The synergistic effect of these two metal oxides enhances the conductivity of the composition.

The plot of variation of specific capacitance with scan rate (**Figure 2(b)**) shows that at lower scan rate the TiO_2-V_2O_5 nanocomposite electrode demonstrate higher capacitance value and it falls with increase of scan rate. This variation can be explained on the basis of movement of ions from electrolyte to electrode material. At lower scan rate, the electrolyte ions get enough time to contact the outer and interior active sites of the material which lead a large number of charge accumulation correspond to high specific capacitance value. Consequently, as the scan rate increase the mobility of charges per unit time increase as well as capacitance decrease due to less number of charge accretions on the outer surface of the electrode material. The charge storage mechanism of the electrode material can be studied according to the Power law, which explains that the total CV current is the sum of non-Faradic capacitive current and adsorptions/desorption currents. According to the Power law, scan rate dependent CV current of the electrode can be written as Eq. (6)

$$i = av^n \tag{6}$$

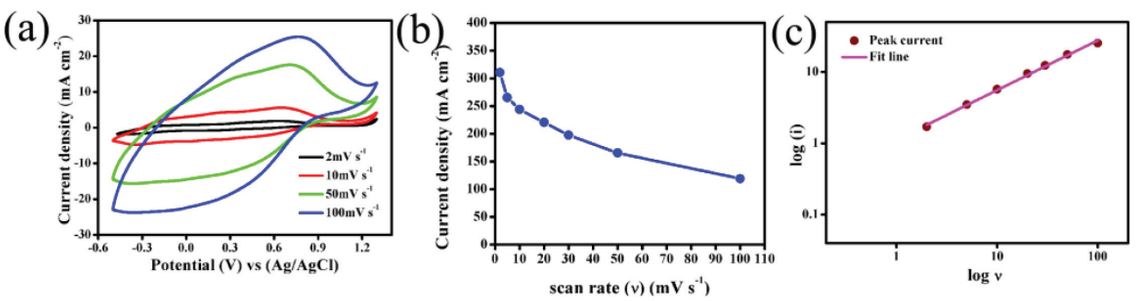

Figure 2.
(a) CV curves at different scan rates; (b) specific capacitance vs. scan rate plot and (c) log(i_p) vs. log(ν) plot for the TiO_2-V_2O_5 composite.

where, 'a' and 'n' are adjustable parameters and ν is scan rate [1, 22]. The value of 'n' can be obtained from slope of the linear fit log(i) vs. log(ν) at a fixed potential. The 'n' value varies from zero to one. For pure resistor n = 0, for ideal diffusion control process n = 0.5 and for ideal capacitive process n = 1.0 i.e. non Faradic process. **Figure 2(c)** shows the plot of log(i) vs. log(ν) of TiO_2-V_2O_5 nanocomposite. For this case, the 'n' value 0.69 reveals that the adsorption/desorption process dominates over capacitive mechanism i.e. the total current can be written as the combination of capacitive and adsorption/desorption current as

$$i = k_1(v) + k_2\left(v^{1/2}\right) \tag{7}$$

where $k_1(\nu)$ and $k_2(\nu^{1/2})$ signify the non-Faradic capacitive current and adsorption/desorption current, respectively. To calculate the value of k_1 and k_2 one can plot $i(V)/\nu^{1/2}$ along y-axis and $\nu^{1/2}$ along x-axis. The slope and intercept of the linear fit gives the values of k_1 and k_2, which can explain the contribution of the Faradic adsorption/desorption current and capacitive current to the total current. It can be concluded that the maximum amount of charge in the working electrode is accumulated based on the adsorption/desorption mechanism instead of capacitive mechanism. On the other hand, Trassati et al. first time reported that the total specific capacitance of an electrode material is the sum of two specific capacitance values provided by the outer and inner surface of the electrode i.e.

$$C_{total} = C_{in} + C_{out}\left(\mathrm{Fg}^{-1}\right) \tag{8}$$

The two specific capacitances due to the influence of inner and outer surface of the electrode strongly depend on the scan rate (ν). The intercept of the linear fit of specific capacitance vs. $\nu^{1/2}$ plot at ν = 0 gives the value of total specific capacitance (320 F g^{-1}) due to the diffusion of ions into the electrode which is nearly equal to the value obtained from CV curve (310 F g^{-1}). Similarly, the value of specific capacitance due to the outer surface of the electrode can be calculated from the plot of total specific capacitance vs. $\nu^{-1/2}$ plot and taking the intercept at $\nu = \infty$ and the value in this case is given by 81 F g^{-1}. Thus it can be concluded that the maximum capacitance value is mainly due to the contribution of inner active sites of the electrode which suggests that the charge storage mechanism is strongly based on adsorption/desorption process rather than capacitive process [1, 24].

To investigate the high performance electrochemical properties and kinetic information of TiO_2-V_2O_5 nanocomposite electrode materials EIS measurements have been done in the frequency range of 0.1 Hz to 100 kHz with AC perturbation amplitude of 10 mV. The EIS plot (**Figure 3(a)**) show frequency dependent three regions which can provide information about the kinetic nature of the electrode material. The small distorted semicircular curve at high frequency is due to the

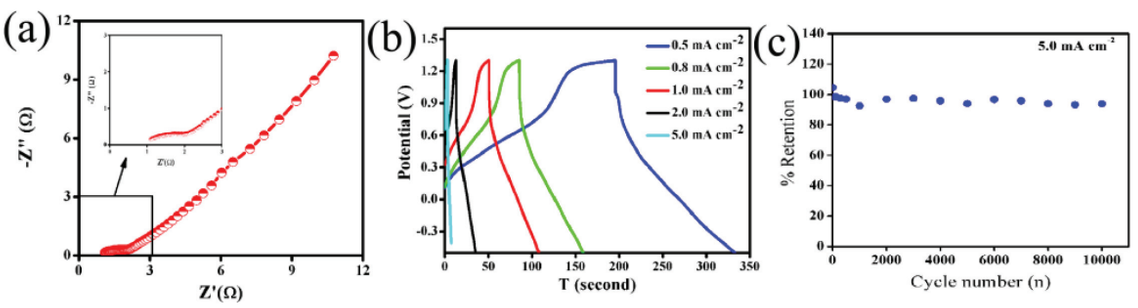

Figure 3.
(a) EIS plot; (b) GCD plot at different current densities and (c) 10000-cycle stability analysis for the TiO_2-V_2O_5 composites.

charge transfer resistance within the electrode material. The diameter of the semi-circular portion gives the value of charge transfer resistance of the material. This semi-circular loop at high frequency can be modeled by a combination of parallel "RC" (R_{ct}-C_{dl}) circuit along with a series resistance (R_s). But, to describe the impedance behavior on the whole frequency range a more detailed circuit have to be considered. Moreover, as seen in FESEM, the electrode materials are particle in nature, the electrolyte can easily access the active material and thus a thin electrolyte film can locally separate the nanoparticles from each other resisting the electronic contact between the materials as well as with the current collector. Because of these two effects the interface resistance R_{ct} is increased. The high frequency loop is formed due to the current collector/ active material interface capacitance C_{dl} in association with the interface resistance R_{ct}. The electrolyte can easily penetrate within the porous electrode materials in the mid frequency range. A straight line corresponding to the frequency dependent Warburg impedance (W) is observed which arises due to the linear diffusion process of ions at the outer surface of the electrode material from electrolyte solution. At very low frequency almost a straight vertical line is observed which mainly originated due to the ions diffusion behavior, indicating very low diffusion resistances.

In order to further study the charge storage ability of synthesized TiO_2-V_2O_5 nanocomposites electrode, GCD at various current densities (0.5, 0.8, 1.0, 2.0 and 5 mA cm^{-2}) has been performed. **Figure 3(b)** represents the GCD plots with potential windows from −0.5 to +1.3 V, which is reliable with the potential range of CV measurement. At lower current densities the composite exhibits good pseudocapacitive behavior and superior capacitive retention. Very small IR drop is also observed at the starting point of discharge time even at high current densities signifies that the electrode material offers very low internal series resistance (R_s) due to the electrolyte solution. However, the sample, due to its mesoporous morphology, accelerated the movement of K^+ and Cl^- ions through its channels inside the pores and reveals superior redox nature at higher current densities. The GCD cycling curves have a nearly symmetric shape at high current densities, indicating that the composite has a good electrochemical capacitive characteristic and superior capacitive retention. The maximum specific capacitance of 307 F g^{-1} has been obtained for TiO_2-V_2O_5 nanocomposites at 0.5 mA cm^{-2} current density, which is almost equal to the value calculated from CV plots. It is also observed that the specific capacitance value decreases with increase of current densities which is mainly due to the decrease of accessibilities of electrolyte ions into the inner surface of the electrode material. The long-term cycle stabilities of prepared TiO_2-V_2O_5 nanocomposite has been studied up to 10,000 cycles at a current density of 5.0 mA cm^{-2} as shown in **Figure 3(c)**. The electrode exhibits very good cycle life of 94% over 10,000 cycles. It has been well explained that both the transition metal oxide play significant role for improvement of excellent electrochemical behavior providing additional possibility of fast redox process even at higher current densities [23, 25].

6.3 Asymmetric supercapacitor device performance

6.3.1 Fabrication of asymmetric supercapacitor

The asymmetric supercapacitor (ASC) was fabricated with activated porous carbon (AC) as negative electrode, TiO_2-V_2O_5 nanocomposite as positive electrode and 1 M Na_2SO_4 as the electrolyte with Whatman filter paper (pore diameter ~25 μm) as separator. The mass ratio of the active materials for negative and positive electrodes was around 2. All the supercapacitive studies of ASCs were

performed at 300 K. The specific energy (E_{cell}) (W h kg^{-1}) and specific power (P_{cell}) (W kg^{-1}) of the device have been calculated by using the Eqs. (9–11)

$$C_s = \frac{I \times \Delta t}{m(V_f - V_i)} \tag{9}$$

$$E_{cell} = \frac{1}{2}\left[\frac{C_s(V_f - V_i)^2}{3.6}\right] \tag{10}$$

$$P_{cell} = \frac{3600 \times E_{cell}}{\Delta t} \tag{11}$$

where C_s is the specific capacitance of the ASC devices (F g^{-1}), I is the discharge current (A), Δt is the discharge time (s), m is the combined mass of the both active electrode materials (g) and (V_f - V_i) is the potential window within which the supercapacitor operate (V) [2]. The cyclic voltammograms (CV) of this fabricated ASCs device have been studied at different potential windows ranging between 0.5 and 1.3 V at a fixed scan rate of 100 mV s^{-1} (**Figure 4(a)**) and it shows no deviation in the shape of the voltammogram at 1.3 V which ensures that the ASC can operate up to 1.3 V. The CV curves of the ASC at different scan rates are shown in **Figure 4(b)**. These curves show the increase of CV current with increasing scan

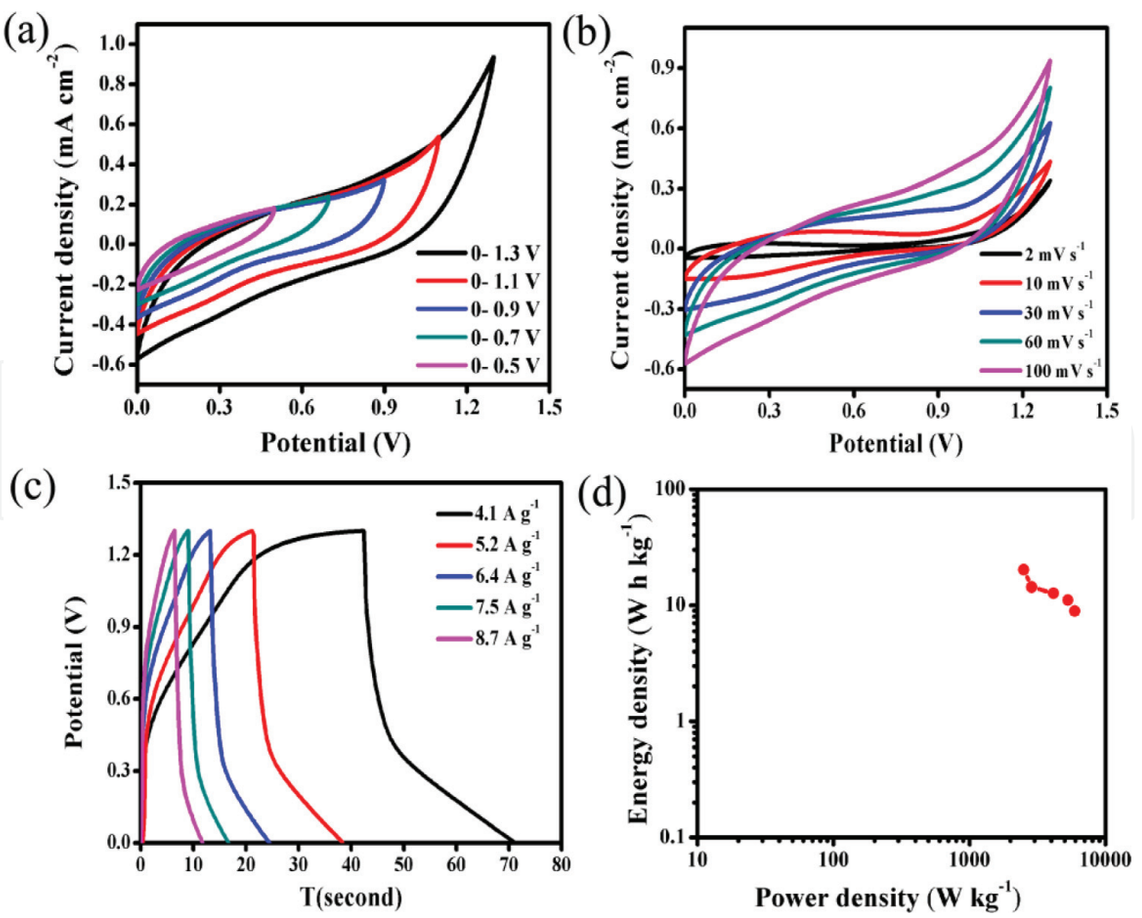

Figure 4.
(a) CV curves at 100 mV s-1 for different window potentials; (b) CV curves at different scan rates for a fixed window; (c) GCD curves at different current densities and (d) energy density vs. power density plot for the TiO_2-V_2O_5 composite device.

rate. The GCD data at different current densities are shown in **Figure 4(c)** and the curves represent that the discharge time decrease with increasing current densities. The specific capacitances were calculated by using Eq. (10) and the value of maximum is 86 F g^{-1} at current density of 4.1 A g^{-1}. From the GCD curves it is clear that the specific capacitance decreases with increase of current densities. The specific energy and specific power of this device have also been calculated using Eqs. (10) and (11) and are shown in the form of Ragone plot in **Figure 4(d)**. The highest specific energy (E_{cell}) and specific power (P_{cell}) is of 20.18 W h kg^{-1} and 5.94 kW kg^{-1}, respectively. Overall electrochemical study of TiO_2-V_2O_5 nanocomposite shows that it is an excellent positive electrode material for future applications.

7. $NiMn_2O_4$ as supercapacitor applications

Recently, single phase spinel-structured $NiMn_2O_4$, a low cost, non-toxic ternary metal oxide, has received a great interests over many other metal oxides due to its excellent electrochemical performance. As has been stated earlier, to be used as electrodes in supercapacitors, materials with good electrical conductivity and excellent electrochemical performance are needed for achieving high energy density and high power density. In this context, nanostructured materials are more suitable than traditional bulk materials as electrode materials for supercapacitor, as they offer higher surface to volume ratio and shorter electron-ions transport channels. In fact, metal oxide nanostructures become the target of modern research for their utilization in high performance energy storage devices. Moreover, the morphology of those nanostructures is seen to affect their electrochemical performance. Therefore, designing metal oxide nanostructures of controlled morphology and size with good electrical conductivity is a challenge for their utilization in energy storage devices such as electrochemical supercapacitors [12, 26].

7.1 Morphological characterization

FESEM image shows (**Figure 5(a)**) densely packed agglomerated spherical $NiMn_2O_4$ nanoparticles of sizes 6–10 nm (~8 nm average size) are formed. Formation of such densely packed small $NiMn_2O_4$ nanoparticles effectively generates

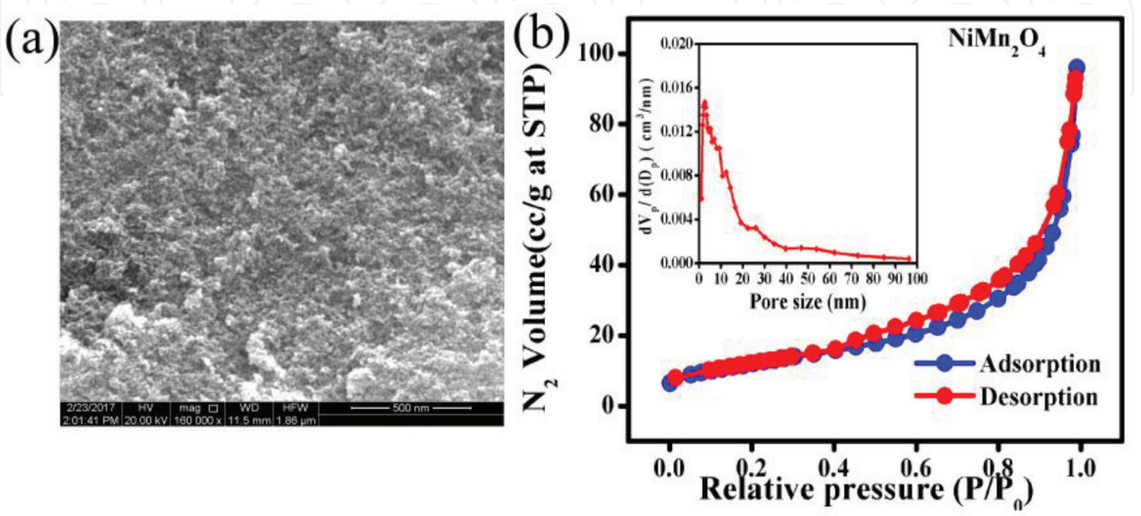

Figure 5.
(a) FESEM image of the $NiMn_2O_4$ nanoparticles; (b) N_2 adsorption-desorption isotherms and pore size distribution curve (inset) of as prepared $NiMn_2O_4$.

porous surface of high specific surface area, which enhances the electrochemical performance of the electrodes due to high contact area of the material with electrolyte. The porous nature of the $NiMn_2O_4$ nanostructures is confirmed form their Brunauer-Emmett-Teller (BET) surface area measurement. The adsorption-desorption plots of the sample presented in **Figure 5(b)** clearly revealed a typical type IV isotherm which corresponds to the mesoporous nature of $NiMn_2O_4$ nanocrystals. The BET estimated specific surface area of the material is 43.6 $m^2\ g^{-1}$ with average pore size 13.3 nm, which offers large number of active sites in the electrochemical process. Such a high specific surface area of the nanostructures can also provide a large contact area between the electrolyte solution and the electrode, ensuing fast ion transfer at the interface.

7.2 Electrochemical characterization

The cyclic voltammogram (CV) curves (**Figure 6(a)**) of the $NiMn_2O_4$ electrode at various scan rates in the potential range −1.0 to 1.3 V indicate the typical Faradic charge transfer behavior due to the presence of functional groups or pore size distribution. The non-rectangular shape of the CV curves specifies the redox nature of the electrode material and provides the information on the pseudocapacitive behavior of the electrode in a suitable electrolyte solution. There are several oxidation and reduction peaks ($Mn^{3+} \leftrightarrow Mn^{4+}$ and $Ni^{2+} \leftrightarrow Ni^{3+}$) in the CV curves, which can be clearly identified due to the faradic redox processes related to Eq. (12) [27].

$$NiMn_2O_4 + Na^+ + e^- \leftrightarrow NaNiMn_2O_4 \tag{12}$$

The specific capacitance (C_m) of the electrode for each scan rate has been calculated from the CV curves by using Eqs. (7) and (8) and the maximum specific capacitance of 875 F g^{-1} is obtained for a scan rate 2 mV s^{-1}. The GCD curves at different current densities (**Figure 6(b)**) indicate the pseudocapacitor type behavior with very low current densities at the potential corresponding to the Faradic reactions. A very small potential drop (IR-drop) has also been observed at the beginning of the discharge curve, even at high current densities, which indicates the $NiMn_2O_4$ electrode has a very low internal series resistance (R_s) within Na_2SO_4 electrolyte solution, as well as low contact resistance at the interface of current collector and electrolyte solution. A decrease of charging/discharging time with increasing current density can be clearly perceived from the GCD curves, which can

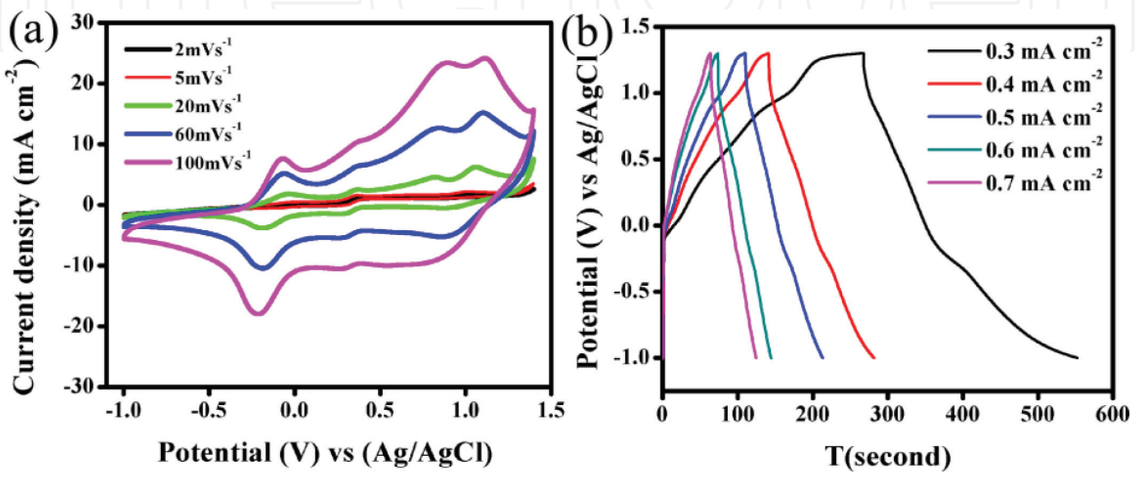

Figure 6.
(a) CV curves at different scan rates and (b) GCD curves at different current densities for the $NiMn_2O_4$ composite.

be explained considering ion diffusion mechanism. At lower current densities, a large surface area of the electrode is occupied by Na^+ ions from electrolyte solution as they get enough time to access the maximum active sites of the electrode material, offering higher specific capacitance value. Conversely, due to limited accessibility of the Na^+ ions inside the electrode material, the specific capacitance of the electrode is lower at higher current densities. The specific capacitance value can also be calculated from the GCD profile at a given current density, using Eq. (8) and the maximum capacitance obtained 820 F g^{-1} at 4.0 A g^{-1}. The electrodes fabricated using $NiMn_2O_4$ nanoparticles exhibit very high cycle life of about 91% over 10,000 cycles, indicating the oxides of both the elements (Ni and Mn) play significant roles for the improvement of electrochemical performance of the electrode.

7.3 Device characterization

It is known that for asymmetric supercapacitors (ASCs) the charge stored at two opposite electrodes (positive and negative) should be equal and opposite i.e. $q^+ = q^-$ [28, 29]. The amount of charge stored by the each electrode generally depends on the specific capacitance (C_m), mass of the electrode (m) and potential windows (ΔV). The ratio of two electrode mass essential to follow:

$$\frac{m_+}{m_-} = \frac{C_- \times (\Delta E)_-}{C_+ \times (\Delta E)_+} \tag{13}$$

Figure 7(a) represents the cyclic voltammograms (CV) of this fabricated ASCs device at different potential windows (0–0.9, 0–1.1, 0–1.3, 0–1.5 and 0–1.8 V). All CV curves show same nature which indicates that this device can performs within

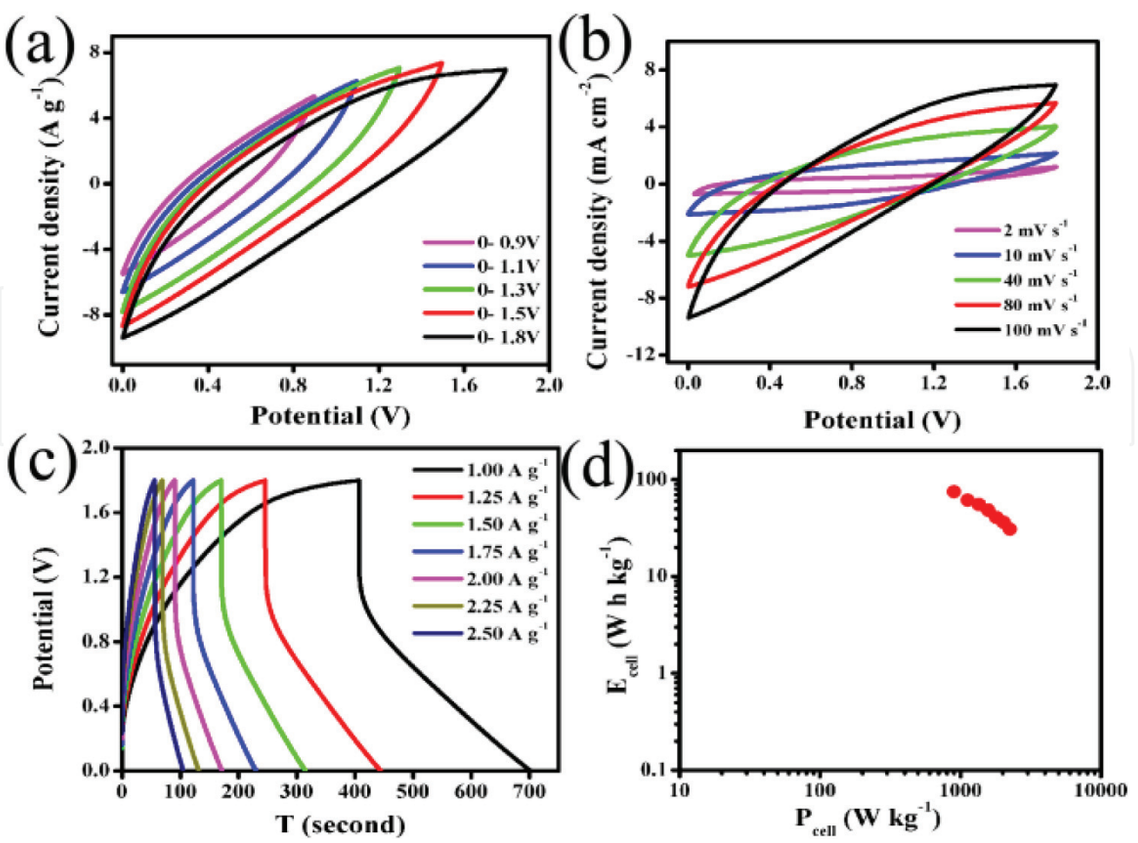

Figure 7.
(a) CV curves at 100 mV s^{-1} for different window potentials; (b) CV curves at different scan rates for a fixed window; (c) GCD curves at different current densities and (d) energy density vs. power density plot for the $NiMn_2O_4$ composite.

maximum potential window 0–1.8 V without any degradation. Thus, all electrochemical studies have been done within maximum potential window from 0 to 1.8 V and the CV curves (**Figure 7(b)**) at different scan rates show relatively rectangular nature without presence of any redox peaks. It clearly indicates that the charge storage mechanism is mainly due to the electric double layer of the device. The CV profiles also remain almost same without any distortion with increasing scan rates, indicating suitable fast charge–discharge property. To study the rate capability of this ASC device, the GCD test at different current densities (1.0, 1.25, 1.50, 1.75, 2.00, 2.25 and 2.50 A g^{-1}) has been performed. The GCD plots (**Figure 7(c)**) show that the discharge time decreases with increasing current density. For practical purpose it is expected that a good supercapacitor device provides high specific capacitance and high energy density. The relationship between specific capacitance vs. current density of the fabricated ASC device shows that the device delivers maximum specific capacitance of 166.7 F g^{-1} at current density 1 A g^{-1}. The specific capacitance also decreases when current density increases, since diffusion of electrolyte ions and electrons most likely are restricted due to the time constrain. The specific energy and power densities of the ASC have been calculated from the discharge curves at different current densities in the voltage window of 0–1.8 V and the Ragone plot is shown in **Figure 7(d)**. This device delivers offers specific energy density and power density of 75.01 W h kg^{-1} and 2.25 kW kg^{-1}, respectively. The ASC device configuration (**Figure 7d**) presents a columbic efficiency 97.6% indicating that the device is suitable for high-performance supercapacitor applications in future.

8. Conclusion

In summary, the electrochemical properties of TiO_2-V_2O_5 and $NiMn_2O_4$ composites have been demonstrated. Three dimensional, mesoporous, interlinked tube-like ordered architecture of TiO_2-V_2O_5 nanocomposite offers large surface area which enhances the specific capacitance. The composite offers maximum specific capacitance of 310 F g^{-1} in 1 M KCl solution at 2 mV s^{-1} scan rate. It is found out that the maximum capacitance value arises from the contribution of inner active sites of the electrode rather than the outer surface. The $NiMn_2O_4$ nanoparticles with ~8 nm average diameter show spherical shape with BET surface area of 43.6 m^2 g^{-1}. The agglomerated spinel nanoparticles generate highly porous structures, which can be utilized to fabricate working electrodes of the electrochemical supercapacitors. The electrodes made of $NiMn_2O_4$ nanoparticles possess excellent charge storage characteristics, with specific capacitance of up to 875 F g^{-1} attainable at a scan rate of 2 mV s^{-1} in 1.0 M Na_2SO_4 electrolyte solution. The coexistence of Ni and Mn in the lattice of this binary oxide is seen to have a positive effect on the improvement of electrochemical charge storage capability of the electrodes due to enhanced electronic conductivity. Both these two composites demonstrate excellent device performance. The asymmetric device based on TiO_2-V_2O_5 shows specific capacity of 86 F g^{-1} at 4.2 A g^{-1} with the maximum energy density (E_{cell}) and power density (P_{cell}) about 20.18 W h kg^{-1} and 5.94 kW kg^{-1}, respectively. On the other hand the asymmetric device based on $NiMn_2O_4$ demonstrates 166.7 F g^{-1} at current density 1 A g^{-1} with specific energy density and power density of 75.01 W h kg^{-1} and 2.25 kW kg^{-1}, respectively. These superior performances ensure that these composites can be used as the electrodes for future energy storage devices.

Acknowledgements

A. Ray (File No.–09/096(0927)/2018-EMR-I) and S. Saha (File No.–09/096 (0898)/2017–EMR-I) wish to thank CSIR, Government of India for financial support. S. Das is thankful to the Department of Science and Technology (DST), Government of India, for providing research support through the 'INSPIRE Faculty Award' (IFA13-PH-71). A. Roy (IF140920) is also thankful to the Department of Science and Technology (DST), INSPIRE, Government of India, for providing research support through the 'INSPIRE Fellowship'.

Conflict of interest

All the authors declare that there is no conflict of interest.

Author details

Apurba Ray, Atanu Roy, Samik Saha and Sachindranath Das*
Department of Instrumentation Science, Jadavpur University, Kolkata, India

*Address all correspondence to: sachindas15@gmail.com

References

[1] Roy A, Ray A, Saha S, Das S. Investigation on energy storage and conversion properties of multifunctional PANI-MWCNT composite. International Journal of Hydrogen Energy. 2018;**43**:7128-7139

[2] Ray A et al. Electrochemical properties of TiO_2-V_2O_5 nanocomposites as a high performance supercapacitors electrode material. Applied Surface Science. 2018;**443**: 581-591

[3] NASA. 2009: Second Warmest Year on Record; End of Warmest Decade. 2010, January 21. [Accessed: November 30, 2010]

[4] Ng CH et al. Cesium lead halide inorganic-based perovskite-sensitized solar cell for photo-supercapacitor application under high humidity condition. ACS Applied Energy Materials. 2018. DOI: 10.1021/acsaem.7b00103

[5] Ngaotrakanwiwat P, Meeyoo V. TiO_2–V_2O_5 nanocomposites as alternative energy storage substances for photocatalysts. Journal of Nanoscience and Nanotechnology. 2012;**12**:828-833

[6] Wang J et al. Nanocellulose-assisted low-temperature synthesis and supercapacitor performance of reduced graphene oxide aerogels. Journal of Power Sources. 2017;**347**:259-269

[7] Jampani PH et al. High energy density titanium doped-vanadium oxide-vertically aligned CNT composite electrodes for supercapacitor applications. Journal of Materials Chemistry A. 2015;**3**:8413-8432

[8] Li X. Improved electrocatalytic activity and durability of $NiMn_2O_4$-CNTs as reversible oxygen reaction electrocatalysts in zinc-air batteries. ECS Transactions (ECST)—The Electrochemical Society. 2017;**80**: 129-134

[9] Conway BE. Electrochemical supercapacitors. Scientific Fundamentals and Technology Applications. Ch 9; 1999

[10] Conway BE. Transition from "supercapacitor" to "battery" behavior in electrochemical energy storage. Journal of the Electrochemical Society. 1991;**138**:1539

[11] Ali GAM, Tan LL, Jose R, Yusoff MM, Chong KF. Electrochemical performance studies of MnO_2 nanoflowers recovered from spent battery. Materials Research Bulletin. 2014;**60**:5-9

[12] Ngo YLT, Sui L, Ahn W, Chung JS, Hur SH. $NiMn_2O_4$ spinel binary nanostructure decorated on three-dimensional reduced graphene oxide hydrogel for bifunctional materials in non-enzymatic glucose sensor. Nanoscale. 2017;**9**:19318-19327

[13] Liu S et al. Nb_2O_5 quantum dots embedded in MOF derived nitrogen-doped porous carbon for advanced hybrid supercapacitor applications. Journal of Materials Chemistry A. 2016;**4**:17838-17847

[14] Rusi, Majid SR. Green synthesis of in situ electrodeposited rGO/MnO_2 nanocomposite for high energy density supercapacitors. Scientific Reports. 2015;**5**:1-13

[15] Vijaya Sankar K et al. Studies on the electrochemical intercalation/de-intercalation mechanism of $NiMn_2O_4$ for high stable pseudocapacitor electrodes. RSC Advances. 2015;**5**: 27649-27656

[16] Tully KC, Whitacre JF, Litster S. Spatiotemporal electrochemical measurements across an electric double layer capacitor electrode with application to aqueous sodium hybrid batteries. Journal of Power Sources. 2014;**248**:348-355

[17] Wu N, Low J, Liu T, Yu J, Cao S. Hierarchical hollow cages of Mn-Co layered double hydroxide as supercapacitor electrode materials. Applied Surface Science. 2017;**413**:35-40

[18] De Pauli CP, Trasatti S. Electrochemical surface characterization of IrO_2 + SnO_2 mixed oxide electrocatalysts. Journal of Electroanalytical Chemistry. 1995;**396**: 161-168

[19] Chen LY, Hou Y, Kang JL, Hirata A, Chen MW. Asymmetric metal oxide pseudocapacitors advanced by three-dimensional nanoporous metal electrodes. Journal of Materials Chemistry A. 2014;**2**:8448-8455

[20] Béguin F, Presser V, Balducci A, Frackowiak E. Carbons and electrolytes for advanced supercapacitors. Advanced Materials. 2014;**26**:2219-2251

[21] Akinwolemiwa B, Peng C, Chen GZ. Redox electrolytes in supercapacitors. Journal of the Electrochemical Society. 2015;**162**:A5054-A5059

[22] Ray A et al. Correlation between the dielectric and electrochemical properties of TiO_2-V_2O_5 nanocomposite for energy storage application. Electrochimica Acta. 2018;**266**:404-413

[23] Roy A et al. NiO-CNT composite for high performance supercapacitor electrode and oxygen evolution reaction. Electrochimica Acta. 2018;**283**: 327-337

[24] Ardizzone S, Fregonara G, Trasatti S. 'Inner' and 'outer' active surface of RuO_2 electrodes. Electrochimica Acta. 1990;**35**:263-267

[25] Lin JY, Huang JJ, Hsueh YL, Zhang YX. Diameter effect of silver nanowire doped in activated carbon as thin film electrode for high performance supercapacitor. Applied Surface Science. 2017. DOI: 10.1016/j.apsusc.2017.10.008

[26] Maiti S, Pramanik A, Dhawa T, Sreemany M, Mahanty S. Bi-metal organic framework derived nickel manganese oxide spinel for lithium-ion battery anode. Materials Science and Engineering: B. 2018;**229**:27-36

[27] Arsent'ev MY, Koval'ko NY, Shmigel' AV, Tikhonov PA, Kalinina MV. $NiMn_2O_4$ spinel as a material for supercapacitors with a pseudocapacity effect. Glass Physics and Chemistry. 2017;**43**:376-379

[28] Li S et al. High-performance flexible asymmetric supercapacitor based on CoAl-LDH and rGO electrodes. Nano-Micro Letters. 2017;**9**:1-10

[29] Wang R, Sui Y, Huang S, Pu Y, Cao P. High-performance flexible all-solid-state asymmetric supercapacitors from nanostructured electrodes prepared by oxidation-assisted dealloying protocol. Chemical Engineering Journal. 2018;**331**: 527-535